HHS Public Access

Author manuscript

J Am Soc Hypertens. Author manuscript; available in PMC 2017 April 01.

Published in final edited form as:

J Am Soc Hypertens. 2016 April ; 10(4): 325–335. doi:10.1016/j.jash.2016.01.019.

Early atherosclerosis aggravates renal microvascular loss and fibrosis in swine renal artery stenosis

Dong Sun, MD, PhD[1,2], **Alfonso Eirin, MD**[1], **Behzad Ebrahimi, PhD**[1], **Stephen C. Textor, MD**[1], **Amir Lerman, MD**[3], and **Lilach O. Lerman, MD, PhD**[1,3]

[1]The Division of Nephrology and hypertension, Mayo Clinic, Rochester, MN, United States

[2]The Department of Nephrology, the affiliated hospital of Xuzhou Medical College, China

[3]The Division of Cardiovascular Disease, Mayo Clinic, Rochester, MN, United States

Abstract

Background—Renal function in patients with atherosclerosis and renal artery stenosis (ARAS) deteriorates more frequently than in non-atherosclerotic RAS. We hypothesized that ARAS aggravates stenotic kidney microvascular loss compared to RAS.

Methods—Domestic pigs were randomized to Normal, RAS, and ARAS (RAS fed a high-cholesterol diet) groups (n=7 each). Ten weeks later stenotic kidney oxygenation, renal blood flow (RBF), and glomerular filtration rate (GFR) were evaluated in-vivo, and microvascular density by Micro-CT.

Results—Blood pressure in both RAS and ARAS was elevated, and stenotic kidney RBF and GFR similarly decreased. RAS decreased the density of small-size cortical microvessels (<200 μm), while ARAS extended the decrease to medium-sized microvessels (200–300 μm). Cortical hypoxia and interstitial fibrosis increased in both RAS and ARAS, but correlated inversely with microvascular density only in RAS.

Conclusions—Atherosclerosis aggravates loss of stenotic-kidney microvessels, yet additional determinants likely contribute to cortical hypoxia and fibrosis in swine ARAS.

Keywords

atherosclerosis; microvascular injury; fibrosis; renal artery stenosis

Contact: Lilach O. Lerman, MD, PhD, Division of Nephrology and Hypertension, Mayo Clinic, 200, First Street SW, Rochester, MN 55905. Fax: (507)-266-9316 Phone: (507)-266-9376, lerman.lilach@mayo.edu.

Disclosure

The authors declare no conflict of interest.

Introduction

Renal artery stenosis (RAS), a narrowing of one or both main renal arteries or their branches, is most commonly caused by atherosclerosis. RAS is an important cause of secondary hypertension in the elderly population,[1] that may ultimately lead to advanced kidney injury.[2] The reported prevalence of clinically manifest atherosclerotic RAS (ARAS) in the Medicare population is approximately 0.5% overall, and 5.5% in those with chronic kidney disease.[3] Because atherosclerotic renovascular disease is often asymptomatic, the true frequency may be higher.[4] Renal dysfunction and hypertension progress in ARAS patients more frequently compared with patients with fibromuscular dysplasia.[5,6] Similarly, we showed that tubular and glomerular dysfunction in ARAS pigs were accentuated compared with RAS alone[7–9]. Yet, the potential effect of ARAS on renal microvascular architecture has not been fully explored.

The renal microcirculation sustains renal perfusion and function, and rarefaction of intrarenal microvessels is an important contributor to renal injury. Loss of microvasculature in various forms of kidney injury correlates directly with the development of glomerular and tubulointerstitial scarring.[10–13], and may lead to chronic ischemia and hypoxia, thus accelerating renal fibrosis.[11] We have previously shown that in ARAS atherogenic factors aggravate renal fibrosis and oxidative stress[7–9]. However, while microvascular rarefaction may also contribute to loss of kidney function distal to RAS[14], the degree to which early atherosclerosis modulates microvascular loss in RAS compared to ARAS remains unclear.

The present study was designed to test the hypothesis that ARAS aggravates stenotic kidney microvascular loss compared to RAS. For this purpose, we compared in swine models of unilateral RAS and ARAS the relationship between the spatial density of microvessels and the impairments in individual kidney hemodynamics, function, oxygenation, and structure.

Materials & Methods

Experimental Design

All procedures were approved by the Institutional Animal Care and Use Committee. Twenty-one female domestic pigs (initially weighing 25–35kg) were randomized to three groups: Normal, RAS and ARAS, which underwent imaging studies after 10 weeks of observation.

In vitro studies were subsequently performed to measure total cholesterol and low-density lipoprotein (LDL) in plasma (Roche), plasma renin activity (Radioimmunoassay, DiaSorin, Stillwater, MN), and serum creatinine (Arbor Assays, Ann Arbor, MI). After completion of all studies, the pigs were euthanized with sodium pentobarbital (100 $mg \cdot kg^{-1}$ IV, Fort Dodge Laboratories). Kidneys were sectioned and immediately shock-frozen in liquid nitrogen and stored at −80°C, pres erved in formalin or prepared for micro-computed tomography (micro-CT).

Induction of RAS and ARAS

Animals were anesthetized with intramuscular Telazol® (Fort Dodge Animal Health, New York, NY) (5mg·kg^{-1}) and xylazine (2mg·kg^{-1}), intubated, and anesthesia maintained with intravenous ketamine (0.2mg·kg^{-1}·min^{-1}) and xylazine (0.03 mg·kg^{-1}·min^{-1}). The femoral artery was catheterized, followed by a heparin bolus (5000U). Under fluoroscopic guidance, local-irritant coils were implanted in the proximal-middle right renal artery, as previously described.[7,14:] RAS pigs were subsequently fed a 10-week standard pig chow (n=7), whereas ARAS consumed an atherogenic diet of 2% cholesterol and 15% lard (TD-93296, Harlan-Teklad) (n=7),[7–9] which is considered a surrogate of early atherosclerosis. In control pigs, selective renal angiography was followed by a 10-week normal diet (Normal, n=7). Mean arterial pressure (MAP) was subsequently measured by a PhysioTel® telemetry system (Data Sciences International, St. Paul, MN) implanted at baseline in the left femoral artery and averaged in the last 2–3 days before study completion.[2,7–9]

Measurement of Kidney Oxygenation

Stenotic kidney oxygenation was determined 10 weeks after the RAS or sham procedure using blood oxygen-level dependent (BOLD) magnetic resonance imaging (MRI) under 1–2% isoflurane inhaled anesthesia. BOLD images were collected at baseline and 15 minutes after injection of a bolus of furosemide (0.5 mg·kg^{-1}), through an ear vein cannula. The renal cortex and medulla were manually traced in each image, and the average relaxivity index R2* computed. The basal BOLD signal (R2*), and its change after furosemide (ΔR2*), were used as measures of tissue oxygenation and oxygen-dependent tubular function, respectively.[15,16]

Measurement of renal function

A few days later after MRI studies, all pigs were again anesthetized and underwent renal angiography. Single-kidney renal blood flow (RBF), glomerular filtration (GFR) and the degree of renal artery stenosis were then evaluated using multidetector CT (MDCT, SOMATOM Definition-64; Siemens, Forchheim, Germany). MDCT images were analyzed with ANALYZE™ (Biomedical Imaging Resource, Mayo Clinic, MN). RBF was calculated by the sum of the products of cortical and medullary perfusions and volumes, and GFR was assessed from the cortical proximal-tubular curve.[17] The degree of stenosis was calculated as the decrease in renal arterial luminal area, as previously described.[2]

Microvascular Architecture

Harvested kidneys were prepared and scanned as previously described.[18] Briefly, Microfil MV122 (an intravascular contrast agent, Flow Tech, Inc.) was perfused under physiological pressure through a cannula ligated in the renal artery. Samples were prepared and scanned at 0.5 degree angular increments at 18-μm resolution, and images analysis was performed with ANALYZE™, as previously described.[18,19] The microvessels (diameters <500 μm) in the renal cortex (divided into equal inner and outer halves) were counted in each level and classified according to diameter as small (20–200 μm), medium (200–300 μm), or large (300–500 μm) microvessels. The medullary microvascular volume fraction (proportion of tissue containing blood vessels) was calculated as previously described.[16]

Kidney Tissue Studies

Renal morphology in each pig was examined in representative 5-μm-thick formalin-embedded sections stained with trichrome. Renal fibrosis was assessed by a computer-aided image analysis program (AxioVision 4.8.2, Carl Zeiss Microscopy, Thornwood, NY). In each slide, trichrome staining was semi-automatically quantified in 6–10 fields, expressed as fraction of kidney surface area, and the results from all fields averaged.[8] Glomerular score (% of sclerotic out of 100 glomeruli) was assessed as described.[20] Tubular injury was scored as described previously.[21] Oxidative stress indicated by *in-situ* production of superoxide anion was quantified in 30 μm fresh frozen tissue slides stained with Dihydroethidium (DHE).[16] Endothelial nitric oxide synthase (eNOS) (1:500; BD Transduction Lab) and phosphorylated eNOS (p-eNOS) (1:500; Abcam) immunofluorescence was also assessed. Nuclear factor-κB (NF-κB, 1:100, Abcam, Cambridge, England) and oxidized low-density lipoprotein (ox-LDL, 1:150, Abcam) immunohistochemistry was done to investigate inflammation and LDL oxidization. Microvascular remodeling, primarily of small and medium-size arteries, was assessed by wall-to-lumen ratio using α-smooth muscle actin (α-SMA) staining (1:50; Dako, Glostrup, Denmark).[22]

Standard Western blotting protocols were followed as described previously,[9,23] using specific antibodies against vascular endothelial growth factor (VEGF, 1:250, Santa-Cruz) and NF-κB (1:1000, Abcam).

Statistical Analysis

Results are shown as mean±SEM. Comparisons among groups were performed by 1-way ANOVA followed by unpaired Student's *t*-tests, and within groups by paired *t*-tests. Least-square regression was used to assess the relationship between renal microvessels, function, and oxygen supply. Statistical significance was accepted for $P \leq 0.05$.

Results

The degree of stenosis and blood pressure were not different between the RAS and ARAS groups (Table 1). MAP in the RAS and ARAS groups increased compared with normal animals ($P=0.05$ and $P=0.02$, respectively), and serum cholesterol and LDL levels were elevated only in ARAS pigs ($P<0.01$ for each). Plasma creatinine was significantly elevated in RAS and ARAS animals compared with Normal ($P=0.02$ and $P=0.01$, respectively), whereas plasma renin activity was not different among the three groups. RBF and GFR were not different between the stenotic RAS and ARAS kidneys and were significantly decreased compared with normal kidneys ($P<0.04$ for each) (Table 1).

Intrarenal Microvasculature

In the renal cortex, RAS decreased the density of small-sized microvessels (<200 μm) through the inner, outer and whole cortex ($P<0.02$ each), while ARAS decreased the density of both small and medium-sized microvessels (200–300 μm) throughout the cortex (Figure 1A and 1B, $P<0.04$ for each). Large microvessels (300–500 μm) remained unchanged in both groups compared to normal kidneys.

In the renal medulla, the density of microvessels in both RAS and ARAS decreased significantly compared to Normal (Figure 1A and 1C, P=0.02 and P=0.007, respectively).

Renal Oxygenation

Basal renal cortical R2*, an index of deoxyhemoglobin concentration in the kidney,[15,24] was higher in both RAS and ARAS than in the Normal group (Figure 1D and 1E, P<0.01 and P<0.05, respectively). Basal medullary R2* values were only elevated in ARAS compared to Normal (Figure 1D and 1E, P=0.04). In response to furosemide, both the cortex and medulla remained more hypoxic in RAS and ARAS than in normal pigs (P<0.04 each). The medullary change in R2* in response to furosemide, as a measure of oxygen-dependent tubular transport function, indicated a similarly attenuated response in both RAS and ARAS compared to Normal (Figure 1D and 1F, P=0.04 and P=0.02, respectively). (Figure 1).

Renal Histology

Stenotic RAS kidneys showed sporadic regions of focal interstitial fibrosis and tubular atrophy, whereas ARAS kidneys showed more extensive multifocal interstitial fibrosis with associated tubular atrophy. Compared with other groups, fibrosis in the ARAS cortex and medulla increased significantly, and was localized mainly in the peritubular interstitial space (Figure 2A and 2B, P≤0.03 each). Glomerular score increased similarly in RAS and ARAS pigs, whereas tubular injury observed in RAS was further aggravated in ARAS (Figure 2A, 2C and 2D, P≤0.05 each). DHE staining was elevated in RAS (P<0.05 vs. Normal), and further exacerbated in ARAS (Figure 2A and 2E, P<0.01 vs. Normal, and P=0.04 vs. RAS). Compared to Normal, total eNOS immunoreactivity decreased in both RAS (P=0.01) and ARAS (Figure 2A and 2F, P=0.006), while p-eNOS decreased only in ARAS (Figure 2A and 2G, P=0.04 vs. Normal). Both ox-LDL and NF-κB immunoreactivities increased significantly only in ARAS kidneys (Figure 3A, 3B and 3C, P≤0.002 vs. Normal and RAS). Microvascular wall thickening (media-to-lumen ratio) increased in RAS (P=0.0001 vs. Normal), but further in ARAS (Figure 3A and 3D, P<0.0001 vs. each).

Western blotting confirmed that NF-κB expression increased significantly only in ARAS (Figure 4A and 4B, P=0.04 vs. Normal, and P=0.04 vs. RAS). VEGF expression was not significantly different among the three groups (Figure 4A and 4C).

Relationship between Microvessels and Stenotic Kidney Function, Oxygenation, and Fibrosis

In the inner and whole cortex, the density of medium microvessels in RAS correlated directly with RBF and GFR (Figure 5). Similarly, the density of medium microvessels in the outer cortex declined with increasing degree of stenosis (data not shown). Contrarily, in ARAS microvascular density did not correlate with the degree of stenosis, RBF or GFR, suggesting that other factors were also involved in renal dysfunction in ARAS. BOLD-MRI showed that in stenotic RAS kidneys, basal renal cortical and medullary R2* (hypoxia index) increased with decreasing density of inner cortical medium-sized microvessels and with medullary vascular volume fraction, respectively. Tubular injury score correlated directly with basal renal cortical R2* in RAS (Figure 5). Furthermore, in stenotic RAS kidneys, medium size microvessels in the whole and inner cortex correlated inversely with

the severity of renal cortical fibrosis and tubular injury score, and medullary microvessels with the severity of medullary fibrosis. On the other hand, in ARAS no such correlation was observed (Figure 5).

Discussion

This study demonstrates that atherosclerosis activates mechanisms that can aggravate loss of stenotic-kidney microvessels beyond the effects of the vascular occlusive lesion alone. Both RAS and ARAS showed cortical hypoxia and marked decreases in RBF and GFR, and eNOS expression, but only in RAS did microvascular loss correlate with these changes. Therefore, additional factors likely contribute to loss of renal function in ARAS.

Atherosclerosis accounts for the majority of cases of clinical RAS. Compared with other causes of RAS, ARAS has unfavorable outcomes,[25] and is increasingly identified in patients with end-stage renal disease.[6] These observations imply that mechanisms beyond the main vessel stenosis contribute to the deleterious effect of hypoperfusion on the kidneys and augment renal damage. Previous studies indicated that atherosclerosis and renal hypoperfusion combine to disrupt the balance among intrarenal vasoactive factors that regulate vascular tone and tissue growth, thereby increasing renal injury.[8] This study extends our previous observations and shows that magnified microvascular loss in ARAS compared to RAS exceeds the level of vascular occlusion and is likely secondary to atherogenic factors.

Accumulating experimental evidence indicates that inflammatory factors play an important role in renal injury in ARAS.[2] In a previous study, we found that stenotic swine kidneys in ARAS have increased tissue levels of the pro-inflammatory chemokine monocyte chemo-attractant protein (MCP-1), which is associated with endothelial dysfunction and microvascular loss.[26] Elevated systemic levels of tumor necrosis factor (TNF)-α and MCP-1 in ARAS patients also persist after revascularization.[27] NF-κB is a transcription factor, which regulates expression of genes involved in inflammation and cell proliferation.[8,28,29] MCP-1/CCR2-dependent activation of NF-κB in tubular epithelial cells might amplify local inflammation[30] and fibrosis. Increased renal tissue inflammation may directly cause microvascular injury and endothelial dysfunction.[31] Hence, upregulation of NF-κB in ARAS pigs might have magnified microvascular injury.

Many forms of renal diseases are associated with increased oxidative stress, and anti-oxidant therapy has been shown to improve renal hemodynamics in experimental renovascular disease[32,33] Furthermore, oxidative stress may contribute to microvascular loss in the stenotic kidney.[18] For example, prolonged and severe tissue inflammation and oxidative stress interfere with upregulation of angiogenic factors.[20,31] Hypoxia increases the expression of many genes, particularly hypoxia-inducible factor (HIF)-1α and VEGF, a major angiogenic factor essential for neovascularization.[34] However, reactive oxygen species may degrade VEGF protein, which may account for its unchanged expression in stenotic kidneys. In the present study, both RAS and ARAS increase renal oxidative stress, as well as a cortical R2* (index of hypoxia), whereas ox-LDL expression increased only in ARAS, possibly also due to increased availability of LDL. Ox-LDL can downregulate

eNOS[35], attenuate its phosphorylation, and thereby aggravate microvascular injury in ARAS compared to RAS, because eNOS is an important effector of VEGF. Furthermore, these were accompanied in ARAS by decreased activation of eNOS, increased immunoreactivity of ox-LDL and NF-κB, as well as oxidative stress and microvascular remodeling, which might be involved in progression of renal injury that characterizes ARAS.

Renal vascular resistance is determined by the integrated components of large interlobar arteries, medium-size arcuate and interlobular arteries, as well as small afferent and efferent arterioles (approximately 40μm in size), capillaries, and veins. Vascular tone in afferent/efferent arterioles and in glomerular capillaries is the main determinant of GFR.[23,36] A decrease in renal hemodynamics in aging results primarily from remodeling of arcuate and interlobular arteries, with an associated interstitial fibrosis.[37] In the inner renal cortex, the frequency of vessels with diameters >250μm, most of which are arcuate and radial vessels[38], increases as the cortico-medullary junction is approached.[39] Interestingly, we observed that in RAS, but not in ARAS, medium-sized cortical microvessels showed a significant linear relationship with RBF, GFR, renal oxygen, fibrosis and tubular injury score, and medullary microvessels correlated inversely with the severity of medullary fibrosis. Indeed, microvascular injury may cause chronic ischemia and hypoxia, and accelerate the process of fibrosis.[11] Basal renal cortical R2* increased in both RAS and ARAS animals, although medullary R2* was elevated only in ARAS, associated with more severe fibrosis. The blunted changes of medullary R2* in RAS and ARAS implied reduced prevailing oxygen consumption related to tubular sodium transport.[2] Moreover, medium-sized microvessels were relatively preserved in RAS compared with Normal pigs, but were decreased in ARAS. We interpret this to indicate that cortical microvessels are critical for maintaining stenotic kidney function in RAS, whereas ARAS activates additional mechanisms that not only aggravate microvascular loss but also impair renal function and structure partly independent of these vascular changes. These changes partly may account for greater decline in renal function in ARAS compared to RAS patients.

Limitations

In our models, RAS and ARAS developed over 10 weeks, with short-term preexisting disease and exposure to atherosclerosis and renovascular disease. Our small sample size might lead to Type-2 errors, and larger studies are also needed to define in greater detail the relationship between kidney function and microcirculation. Notably, despite the divergent relationship of microvascular density with renal function, differences in hemodynamics, function, or glomerulosclerosis between RAS and ARAS kidneys were not significant. Possibly, longer duration of ARAS might impose functionally more severe kidney damage, likely related to ischemia. We have previously found that an atherosclerotic diet induces only mild functional and structural changes in kidney[7–9], with no insulin resistance Notably, microvascular density assessed ex-vivo with micro-CT might be slightly different from that observed in-vivo, yet likely reflects availability of microvessels. While not statistically significantly different, we cannot rule out the possibility of the small differences in body weight and blood pressure in ARAS compared to RAS modulated injury. In addition,

because of the vascular complexity of the kidney, arbitrary division of the cortex into halves may have no anatomical correlate in terms of vascular pattern.[40]

In conclusion, the present study demonstrates that atherosclerosis aggravates loss of cortical microvessels. Nevertheless, while in stenotic-kidneys in non-atherosclerotic RAS renal remodeling and dysfunction may be attributable to microvascular loss, in ARAS additional factors may magnify progression of kidney injury, including inflammation, oxidative stress, and LDL oxidation, which promote development of renal fibrosis. Although at this early stage renal function and hemodynamics in ARAS decreased to the same extent as in RAS, greater renal injury is likely to accelerate deterioration of renal function at a more advanced phase and increase its vulnerability to additional co-existing risk factors. These deleterious alterations may account for accelerated renal dysfunction observed in atherosclerotic renovascular disease, and warrant a multi-pronged approach tailored for underlying mechanisms in order to halt progressive loss of renal function.

Acknowledgments

This study was partly supported by NIH Grant numbers DK73608, HL121561, DK100081, DK104273, and HL123160.

We thank the funding of Jiangsu Overseas & Training Program for University Prominent Young & Middle-aged Teachers and Presidents, project of key medical personnel of Jiangsu Province (RC2011116), and project of National Natural Science Foundation of China (81270769).

References

1. Hansen KJ, Edwards MS, Craven TE, Cherr GS, Jackson SA, Appel RG, Burke GL, Dean RH. Prevalence of renovascular disease in the elderly: a population-based study. Journal of vascular surgery. 2002; 36(3):443–451. [PubMed: 12218965]
2. Eirin A, Ebrahimi B, Zhang X, Zhu XY, Tang H, Crane JA, Lerman A, Textor SC, Lerman LO. Changes in Glomerular Filtration Rate After Renal Revascularization Correlate With Microvascular Hemodynamics and Inflammation in Swine Renal Artery Stenosis. Circulation: Cardiovascular Interventions. 2012; 5(5):720–728. [PubMed: 23048054]
3. Kalra PA, Guo H, Kausz AT, Gilbertson DT, Liu J, Chen SC, Ishani A, Collins AJ, Foley RN. Atherosclerotic renovascular disease in United States patients aged 67 years or older: risk factors, revascularization, and prognosis. Kidney Int. 2005; 68(1):293–301. [PubMed: 15954920]
4. Dworkin LD, Cooper CJ. Clinical practice. Renal-artery stenosis. N Engl J Med. 2009; 361(20): 1972–1978. [PubMed: 19907044]
5. Dejani H, Eisen TD, Finkelstein FO. Revascularization of renal artery stenosis in patients with renal insufficiency. Am J Kidney Dis. 2000; 36(4):752–758. [PubMed: 11007677]
6. Morganti A. Angioplasty of the renal artery: antihypertensive and renal effects. J Nephrol. 2000; 13(Suppl 3):S28–S33. [PubMed: 11132030]
7. Urbieta-Caceres VH, Lavi R, Zhu XY, Crane JA, Textor SC, Lerman A, Lerman LO. Early atherosclerosis aggravates the effect of renal artery stenosis on the swine kidney. American journal of physiology. 2010; 299(1):F135–F140. [PubMed: 20462971]
8. Chade AR, Rodriguez-Porcel M, Grande JP, Krier JD, Lerman A, Romero JC, Napoli C, Lerman LO. Distinct renal injury in early atherosclerosis and renovascular disease. Circulation. 2002; 106(9):1165–1171. [PubMed: 12196346]
9. Chade AR, Rodriguez-Porcel M, Grande JP, Zhu X, Sica V, Napoli C, Sawamura T, Textor SC, Lerman A, Lerman LO. Mechanisms of renal structural alterations in combined hypercholesterolemia and renal artery stenosis. Arterioscler Thromb Vasc Biol. 2003; 23(7):1295–1301. [PubMed: 12750121]

10. Kang DH, Kanellis J, Hugo C, Truong L, Anderson S, Kerjaschki D, Schreiner GF, Johnson RJ. Role of the microvascular endothelium in progressive renal disease. J Am Soc Nephrol. 2002; 13(3):806–816. [PubMed: 11856789]
11. Sun D, Bu L, Liu C, Yin Z, Zhou X, Li X, Xiao A. Therapeutic effects of human amniotic fluid-derived stem cells on renal interstitial fibrosis in a murine model of unilateral ureteral obstruction. PLoS One. 2013; 8(5):e65042. [PubMed: 23724119]
12. Sun D, Wang Y, Liu C, Zhou X, Li X, Xiao A. Effects of nitric oxide on renal interstitial fibrosis in rats with unilateral ureteral obstruction. Life Sci. 2012; 90(23–24):900–909. [PubMed: 22572614]
13. Sun D, Feng J, Dai C, Sun L, Jin T, Ma J, Wang L. Role of peritubular capillary loss and hypoxia in progressive tubulointerstitial fibrosis in a rat model of aristolochic acid nephropathy. Am J Nephrol. 2006; 26(4):363–371. [PubMed: 16873992]
14. Favreau F, Zhu XY, Krier JD, Lin J, Warner L, Textor SC, Lerman LO. Revascularization of swine renal artery stenosis improves renal function but not the changes in vascular structure. Kidney Int. 2010; 78(11):1110–1118. [PubMed: 20463652]
15. Warner L, Glockner JF, Woollard J, Textor SC, Romero JC, Lerman LO. Determinations of renal cortical and medullary oxygenation using blood oxygen level-dependent magnetic resonance imaging and selective diuretics. Investigative radiology. 2011; 46(1):41–47. [PubMed: 20856128]
16. Ebrahimi B, Eirin A, Li Z, Zhu XY, Zhang X, Lerman A, Textor SC, Lerman LO. Mesenchymal stem cells improve medullary inflammation and fibrosis after revascularization of Swine atherosclerotic renal artery stenosis. PLoS One. 2013; 8(7):e67474. [PubMed: 23844014]
17. Daghini E, Primak AN, Chade AR, Krier JD, Zhu XY, Ritman EL, McCollough CH, Lerman LO. Assessment of renal hemodynamics and function in pigs with 64-section multidetector CT: comparison with electron-beam CT. Radiology. 2007; 243(2):405–412. [PubMed: 17456868]
18. Zhu XY, Rodriguez-Porcel M, Bentley MD, Chade AR, Sica V, Napoli C, Caplice N, Ritman EL, Lerman A, Lerman LO. Antioxidant intervention attenuates myocardial neovascularization in hypercholesterolemia. Circulation. 2004; 109(17):2109–2115. [PubMed: 15051643]
19. Zhang X, Eirin A, Li ZL, Crane JA, Krier JD, Ebrahimi B, Pawar AS, Zhu XY, Tang H, Jordan KL, Lerman A, Textor SC, Lerman LO. Angiotensin receptor blockade has protective effects on the poststenotic porcine kidney. Kidney Int. 2013; 84(4):767–775. [PubMed: 23615504]
20. Chade AR, Zhu X, Lavi R, Krier JD, Pislaru S, Simari RD, Napoli C, Lerman A, Lerman LO. Endothelial progenitor cells restore renal function in chronic experimental renovascular disease. Circulation. 2009; 119(4):547–557. [PubMed: 19153272]
21. Nangaku M, Alpers CE, Pippin J, Shankland SJ, Kurokawa K, Adler S, Morgan BP, Johnson RJ, Couser WG. CD59 protects glomerular endothelial cells from immune-mediated thrombotic microangiopathy in rats. J Am Soc Nephrol. 1998; 9(4):590–597. [PubMed: 9555661]
22. Sun D, Eirin A, Zhu XY, Zhang X, Crane JA, Woollard JR, Lerman A, Lerman LO. Experimental coronary artery stenosis accelerates kidney damage in renovascular hypertensive swine. Kidney Int. 2014
23. Eirin A, Zhu XY, Urbieta-Caceres VH, Grande JP, Lerman A, Textor SC, Lerman LO. Persistent kidney dysfunction in swine renal artery stenosis correlates with outer cortical microvascular remodeling. American journal of physiology. 2011; 300(6):F1394–F1401. [PubMed: 21367913]
24. Ebrahimi B, Gloviczki M, Woollard JR, Crane JA, Textor SC, Lerman LO. Compartmental analysis of renal BOLD MRI data: introduction and validation. Investigative radiology. 2012; 47(3):175– 182. [PubMed: 22183077]
25. Safian RD, Textor SC. Renal-artery stenosis. N Engl J Med. 2001; 344(6):431–442. [PubMed: 11172181]
26. Eirin A, Gloviczki ML, Tang H, Gossl M, Jordan KL, Woollard JR, Lerman A, Grande JP, Textor SC, Lerman LO. Inflammatory and injury signals released from the post-stenotic human kidney. European Heart Journal. 2012; 34(7):540–548. [PubMed: 22771675]
27. Saad A, Herrmann SM, Crane J, Glockner JF, McKusick MA, Misra S, Eirin A, Ebrahimi B, Lerman LO, Textor SC. Stent revascularization restores cortical blood flow and reverses tissue hypoxia in atherosclerotic renal artery stenosis but fails to reverse inflammatory pathways or glomerular filtration rate. Circulation Cardiovascular interventions. 2013; 6(4):428–435. [PubMed: 23899868]

28. Chade AR, Bentley MD, Zhu X, Rodriguez-Porcel M, Niemeyer S, Amores-Arriaga B, Napoli C, Ritman EL, Lerman A, Lerman LO. Antioxidant intervention prevents renal neovascularization in hypercholesterolemic pigs. J Am Soc Nephrol. 2004; 15(7):1816–1825. [PubMed: 15213269]
29. Chade AR, Rodriguez-Porcel M, Herrmann J, Zhu X, Grande JP, Napoli C, Lerman A, Lerman LO. Antioxidant Intervention Blunts Renal Injury in Experimental Renovascular Disease. J Am Soc Nephrol. 2004; 15(4):958–966. [PubMed: 15034098]
30. Viedt C, Dechend R, Fei J, Hansch GM, Kreuzer J, Orth SR. MCP-1 induces inflammatory activation of human tubular epithelial cells: involvement of the transcription factors, nuclear factor-kappaB and activating protein-1. J Am Soc Nephrol. 2002; 13(6):1534–1547. [PubMed: 12039983]
31. Chade AR, Zhu X, Mushin OP, Napoli C, Lerman A, Lerman LO. Simvastatin promotes angiogenesis and prevents microvascular remodeling in chronic renal ischemia. Faseb J. 2006; 20(10):1706–1708. [PubMed: 16790524]
32. Welch WJ, Mendonca M, Aslam S, Wilcox CS. Roles of oxidative stress and AT1 receptors in renal hemodynamics and oxygenation in the postclipped 2K,1C kidney. Hypertension. 2003; 41(3 Pt 2):692–696. [PubMed: 12623981]
33. Chade AR, Rodriguez-Porcel M, Herrmann J, Krier JD, Zhu X, Lerman A, Lerman LO. Beneficial Effects of Antioxidant Vitamins on the Stenotic Kidney. Hypertension. 2003; 42(4):605–612. [PubMed: 12925565]
34. Zhu XY, Daghini E, Chade AR, Lavi R, Napoli C, Lerman A, Lerman LO. Disparate effects of simvastatin on angiogenesis during hypoxia and inflammation. Life Sci. 2008; 83(23–24):801–809. [PubMed: 18976673]
35. Zhou J, Abid MD, Xiong Y, Chen Q, Chen J. ox-LDL downregulates eNOS activity via LOX-1-mediated endoplasmic reticulum stress. Int J Mol Med. 2013; 32(6):1442–1450. [PubMed: 24085225]
36. Microvascular Disease. In: Chade, AR., editor; Lilach, O.; Lerman, SCT., editors. Renal Vascular Disease. London: Springer; 2014. p. 362
37. Fuiano G, Sund S, Mazza G, Rosa M, Caglioti A, Gallo G, Natale G, Andreucci M, Memoli B, De Nicola L, Conte G. Renal hemodynamic response to maximal vasodilating stimulus in healthy older subjects. Kidney Int. 2001; 59(3):1052–1058. [PubMed: 11231360]
38. Zhu XY, Chade AR, Rodriguez-Porcel M, Bentley MD, Ritman EL, Lerman A, Lerman LO. Cortical microvascular remodeling in the stenotic kidney: role of increased oxidative stress. Arterioscler Thromb Vasc Biol. 2004; 24(10):1854–1859. [PubMed: 15308558]
39. Xu LX, Holmes KR, Moore B, Chen MM, Arkin H. Microvascular architecture within the pig kidney cortex. Microvasc Res. 1994; 47(3):293–307. [PubMed: 8084296]
40. Beeuwkes R 3rd. The vascular organization of the kidney. Annu Rev Physiol. 1980; 42:531–542. [PubMed: 6996596]

Highlights

- RAS and ARAS induce similar hypertension and stenotic kidney dysfunction.
- Swine ARAS magnifies loss of stenotic kidney cortical microvessels.
- Cortical hypoxia and fibrosis do not correlate with microvascular loss in RAS.
- In swine ARAS determinants additional to RAS alone contribute to cortical injury.

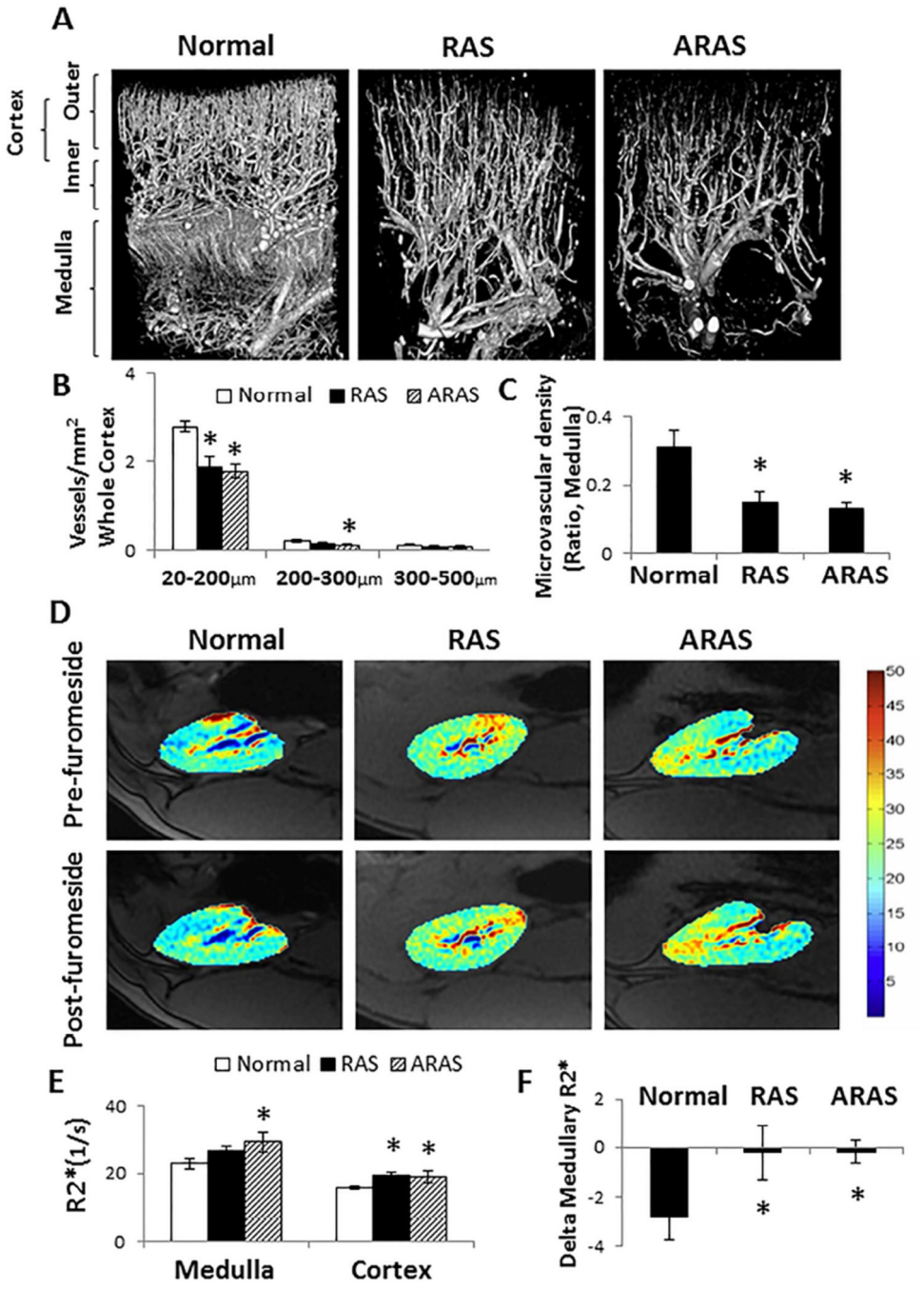

Figure 1.

Renal microvasculature and oxygenation in Normal, renal artery stenosis (RAS), and atherosclerotic RAS (ARAS) pigs. A. Representative micro-CT images. B. In the renal cortex, RAS decreased the density of small-sized microvessels (<200 μm) throughout the whole cortex, while ARAS decreased the density of both small and medium-sized (200–300 μm) microvessels. C. Medullary microvessels decreased in both RAS and ARAS compared with Normal. D. Representative BOLD images. E. Basal renal cortical R2* increased in both RAS and ARAS compared with Normal, but medullary R2* were only elevated in ARAS. F.

The medullary R2* response to furosemide was blunted in both RAS and ARAS. $^{*}P<0.05$ vs. Normal; $^{\#}P<0.05$ vs. RAS.

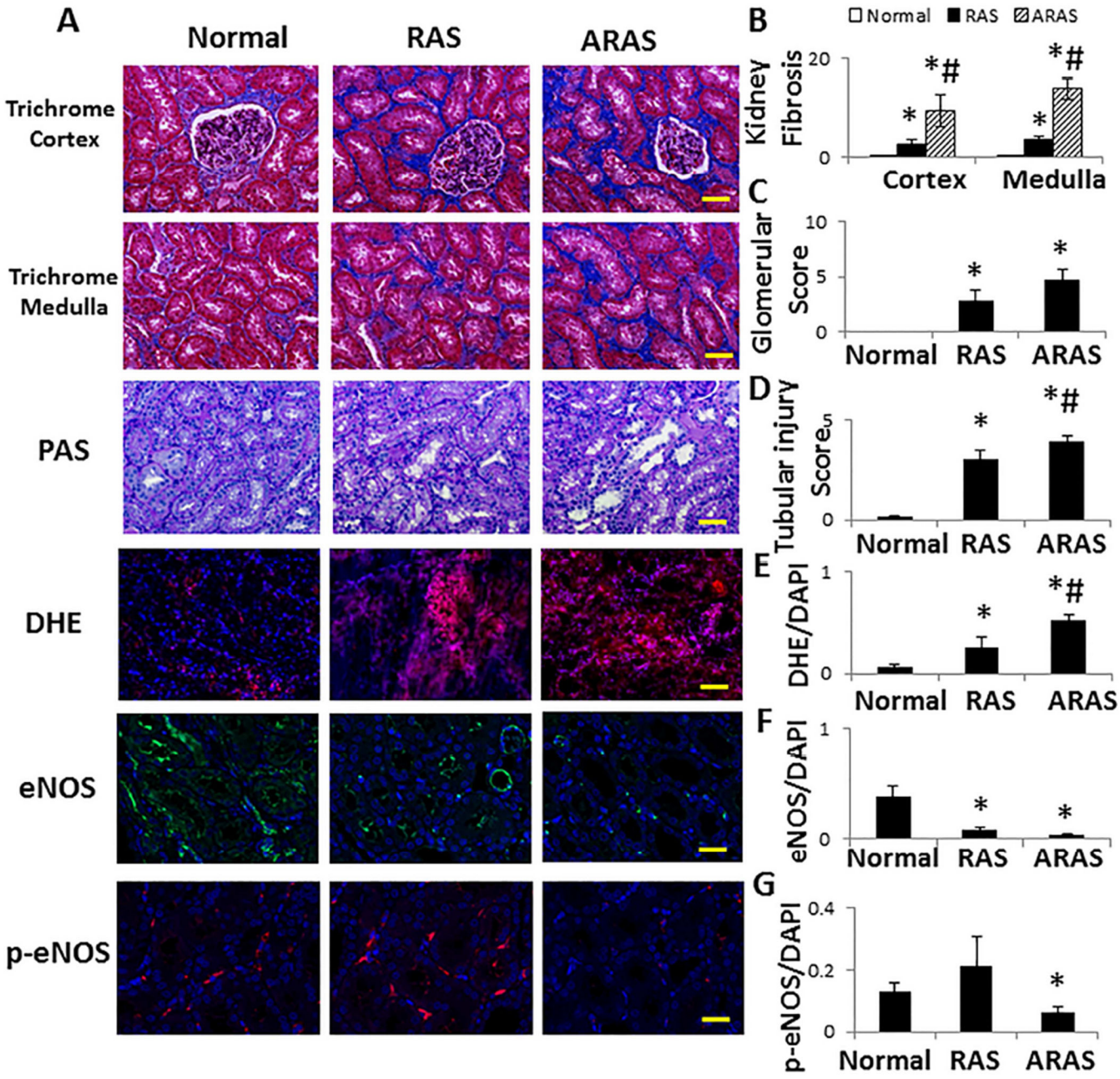

Figure 2.

Renal tissue remodeling. A. Representative renal trichrome, dihydroethidium (DHE), eNOS and p-eNOS immunofluorescence (all ×20). B. Renal cortical and medullary fibrosis increased in RAS compared with Normal, and aggravated in ARAS. C. Glomerular score increased in RAS and ARAS. D. Tubular injury score increased in RAS, and further aggravated in ARAS. E. DHE staining (normalized to DAPI-positive nuclei) increased in RAS compared with Normal, and in ARAS compared with Normal and RAS. F–G. eNOS expression decreased in RAS and ARAS compared with Normal, but p-eNOS only decreased in ARAS. $^{*}P<0.05$ vs. Normal; $^{\#}P<0.05$ vs. RAS. Scale bar=50 μm.

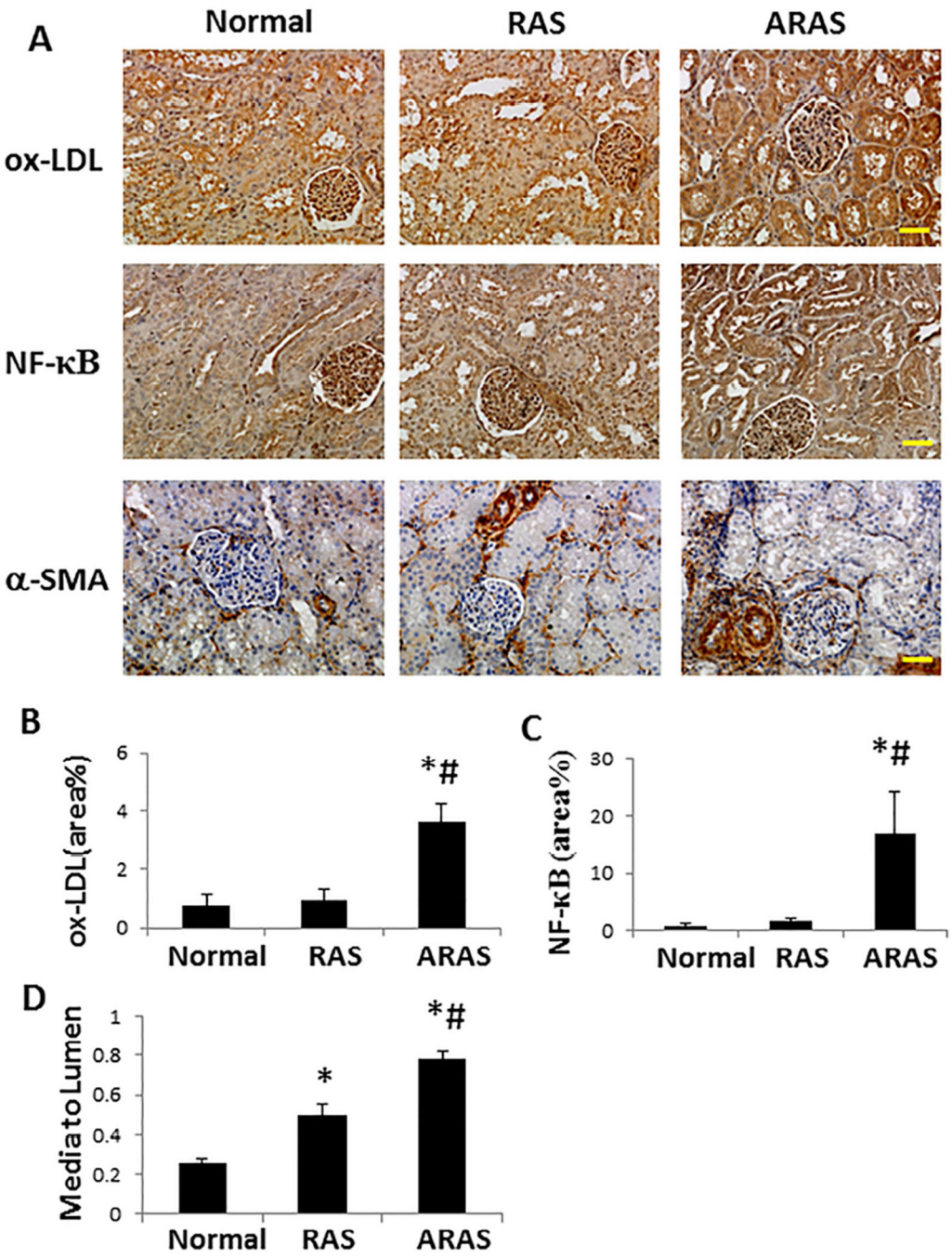

Figure 3.

Immunohistochemical staining. A. Representative ox-LDL, NF-κB and α-SMA staining (all ×20). B, C. ox-LDL and NF-κB immunoreactivity increased in ARAS compared with both Normal and RAS. D. Renal microvascular media-to-lumen ratio (α-SMA) increased in RAS compared with Normal, and further in ARAS compared with Normal and RAS. $^{*}P<0.05$ vs. Normal; $^{\#}P<0.05$ vs. RAS. Scale bar=50 μm.

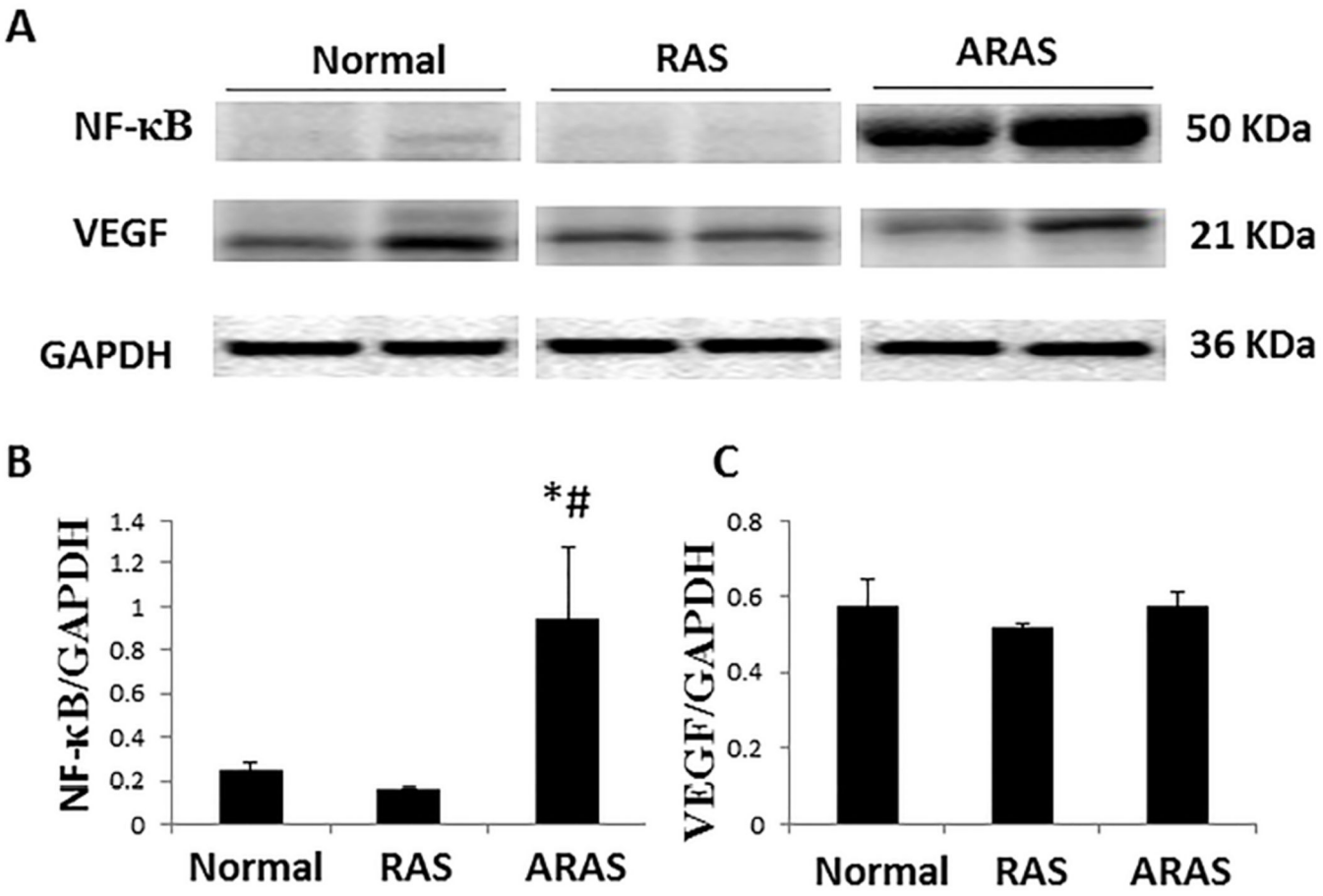

Figure 4.

NF-κB and VEGF expression. A. Western blotting (representative 2 bands shown per group) in three groups. B, C. NF-κB increased in ARAS compared with Normal and RAS, but VEGF expression was not significantly different among the three groups. $^{*}P<0.05$ vs. Normal; $^{\#}P<0.05$ vs. RAS.

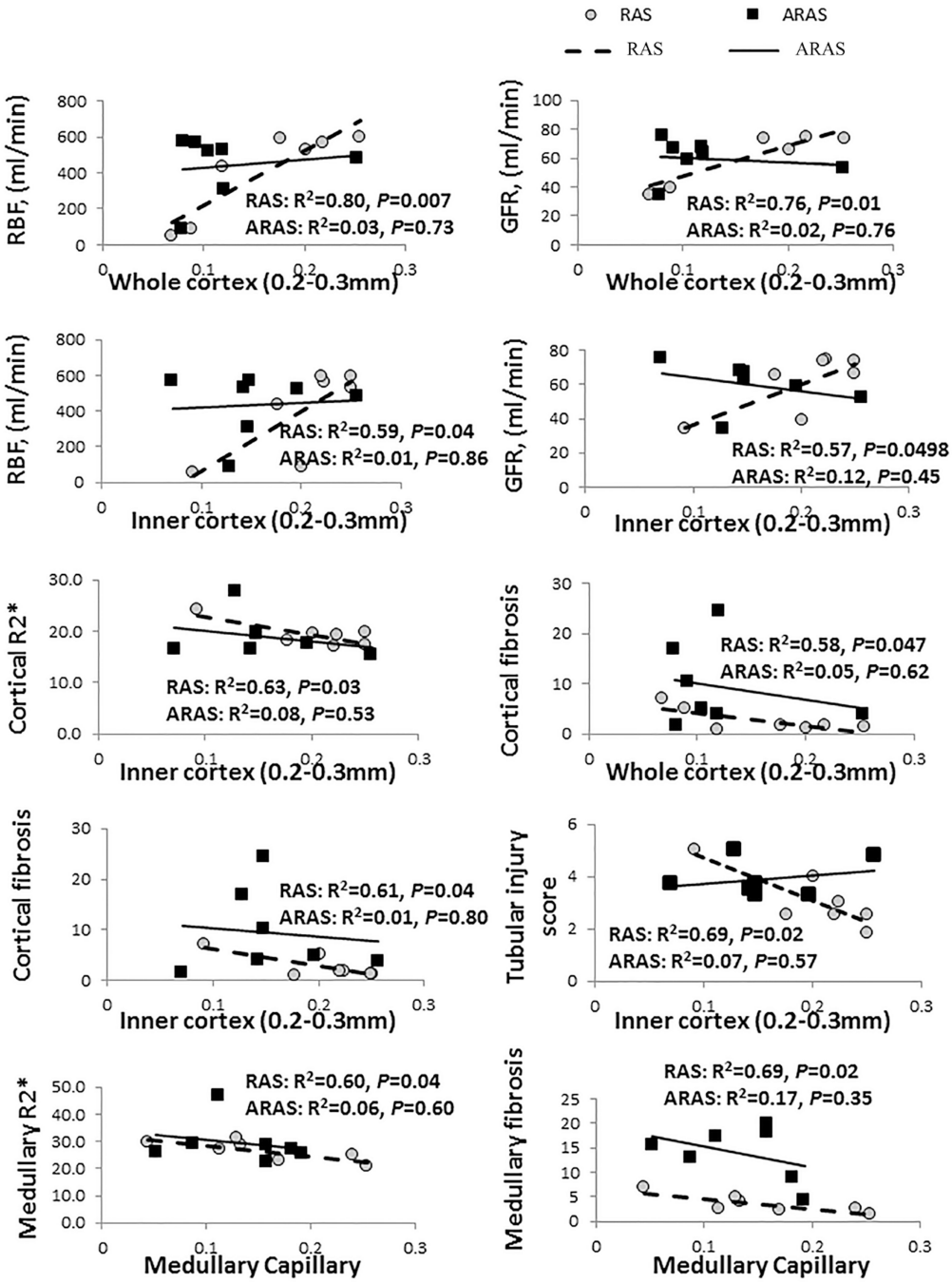

Figure 5.

Correlation of cortical medium-sized microvessels and medullary microvessels with RBF, GFR, cortical and medullary R2*, tubular injury score and fibrosis.

Table 1

Systemic characteristics, single-kidney hemodynamics and function in Normal, renal artery stenosis (RAS) and atherosclerotic RAS (ARAS) pigs (mean±SEM).

	Normal (n=7)	RAS (n=7)	ARAS (n=7)
Body weight, kg	48.2±1.2	48.7±4.1	52.1±2.2
Degree of renal artery stenosis, %	0	76.0±7.2 *	68.9±8.0 *
MAP, mmHg	98.4±1.6	117.5±10.7 *	127.4±10.9 *
Total Cholesterol, mg/dl	82.3±3.6	88.2±7.9	405.3±59.7 *#
LDL, mg/dl	31.1±2.7	38.5±1.8	248.4±42.9 *#
Creatinine, mg/dl	1.20±0.13	1.68±0.11 *	1.73±0.03 *
Plasma renin activity, ng/mL/h	0.11±0.03	0.20±0.08	0.16±0.03
STK RBF, min/min	640.0±45.1	405.5±90.0 *	436.7±67.7 *
STK GFR, ml/min	87.9±7.8	60.6±6.4 *	59.6±5.0 *

MAP, mean arterial pressure; LDL, low density lipoprotein; RBF, renal blood flow; GFR, glomerular filtration rate; STK, stenotic kidney.

* $P<0.05$ vs. Normal;

# $P<0.05$ vs. RAS.